

ISSN 2686-7575 (Online)

<https://doi.org/10.32362/2410-6593-2023-18-6-517-533>



UDC 548.03+53.092+539.26+535.375.54

RESEARCH ARTICLE

Effect of adding technologically processed antibodies to interferon-gamma into a parent solution on the structural features of triglycine sulfate crystals grown from this solution

German O. Stepanov¹, Natalia N. Rodionova^{1,✉}, Roman R. Konstantinov¹, Kirill A. Subbotin^{2,3}

¹Materia Medica Holding, Moscow, 129172 Russia

²Prokhorov General Physics Institute of the Russian Academy of Sciences, Moscow, 119991 Russia

³Mendeleev University of Chemical Technology of Russia, Moscow, 125047 Russia

✉ Corresponding author, e-mail: rodionovann@materiamedica.ru

Abstract

Objectives. Ferroelectric triglycine sulfate (TGS) belongs to a group of crystals whose properties are sensitive even to minor changes in growth conditions. The mechanism of spontaneous polarization in TGS is associated with the adjustment of protons which participate in the formation of hydrogen bonds. Therefore, the state of the parent solution plays an important role in the crystal formation. The study aims to investigate the structural features of TGS crystals grown using aqueous alcoholic solutions of technologically processed antibodies to interferon-gamma, in comparison with those of the crystals grown using the control solutions (technologically processed phosphate-buffered saline and intact aqueous alcoholic solution).

Methods. X-ray diffraction assay and Raman spectroscopy.

Results. The effect of solutions of the technologically processed antibodies to interferon-gamma added to a parent solution on the growth of TGS single crystals is established. This effect manifests in the changing in occupancy of the proton sublattice of the crystal grown from the parent solution containing technologically processed antibodies to interferon-gamma, as compared with the crystals grown from the control solutions. In the case of the crystal grown from the solution containing technologically processed antibodies to interferon-gamma, this change in the occupancy of the proton lattice is expressed in an increase in the length of N2–C3 bonds.

Conclusions. Adding the technologically processed antibodies in the parent solution before the crystal growth can affect the structure of TGS crystals.

Keywords: technologically processed antibodies, triglycine sulfate, single crystal, X-ray diffraction assay, Raman spectroscopy

For citation: Stepanov G.O., Rodionova N.N., Konstantinov R.R., Subbotin K.A. Effect of adding technologically processed antibodies to interferon-gamma into a parent solution on the structural features of triglycine sulfate crystals grown from this solution. *Tonk. Khim. Tekhnol. = Fine Chem. Technol.* 2023;18(6):517–533. <https://doi.org/10.32362/2410-6593-2023-18-6-517-533>

НАУЧНАЯ СТАТЬЯ

Влияние добавления в маточный раствор технологически отработанных антител к интерферону-гамма на структурные особенности выращиваемых из этого раствора кристаллов триглицинсульфата

Г.О. Степанов¹, Н.Н. Родионова^{1,✉}, Р.Р. Константинов¹, К.А. Субботин^{2,3}

¹НПФ «МАТЕРИА МЕДИКА ХОЛДИНГ», Москва, 129172 Россия

²Институт общей физики им. А.М. Прохорова РАН, Москва, 119991 Россия

³Российский химико-технологический университет им. Д.И. Менделеева, Москва, 125047 Россия

✉ Автор для переписки, e-mail: rodionovann@materiamedica.ru

Аннотация

Цели. Сегнетоэлектрик триглицинсульфат (ТГС) относится к группе кристаллов, свойства которых чувствительны даже к незначительным изменениям условий получения. Механизм возникновения спонтанной поляризации в ТГС связан с упорядочением протонов, участвующих в образовании водородных связей, поэтому при формировании кристалла важна роль состояния маточного водного раствора. Цель работы — изучить структурные особенности кристаллов ТГС, выращенных с применением водно-спиртового раствора технологически обработанных антител

к интерферону-гамма, по сравнению с таковыми у кристаллов, выращенных с применением контрольных растворов (технологически-обработанного раствора фосфатно-солевого буфера и интактного водно-спиртового раствора).

Методы. Рентгеноструктурный анализ и спектроскопия комбинационного рассеяния света.

Результаты. Показано влияние растворов технологически обработанных антител к интерферону-гамма, применявшихся при изготовлении маточных растворов, использованных при выращивании кристаллов ТГС, на структурные особенности этих кристаллов. Данное влияние выражается в изменении заселенностей протонной подрешетки кристаллов, выращенных из раствора, содержащего технологически обработанные антитела к интерферону-гамма, по сравнению с кристаллами, выращенными из контрольных растворов, и проявляется в увеличении длины связей N2–C3.

Выводы. Добавление технологически обработанных антител к маточному раствору, используемому для выращивания кристаллов, способно оказывать влияние на структуру кристаллов ТГС.

Ключевые слова: технологически обработанные антитела, триглицинсульфат, кристалл, рентгеноструктурный анализ, спектроскопия комбинационного рассеяния света

Для цитирования: Степанов Г.О., Родионова Н.Н., Константинов Р.Р., Субботин К.А. Влияние добавления в маточный раствор технологически обработанных антител к интерферону-гамма на структурные особенности выращиваемых из этого раствора кристаллов триглицинсульфата. *Тонкие химические технологии.* 2023;18(6):517–533. <https://doi.org/10.32362/2410-6593-2023-18-6-517-533>

INTRODUCTION

Triglycine sulfate (TGS) is a well-known ferroelectric which finds wide application in electronics and other fields. The properties of ferroelectrics are sensitive to even slight variations in synthesis conditions [1]. TGS consists of three glycine molecules and one sulfate anion. Glycine, due to its amphoteric nature, presents positively charged glycinium cations $\text{NH}_3^+\text{CH}_2\text{COOH}$ in acidic solutions, negatively charged anions $\text{NH}_2\text{CH}_2\text{COO}^-$ in alkaline solutions, and bipolar zwitterions $\text{NH}_3^+\text{CH}_2\text{COO}^-$ in a neutral medium. Thus, two glycinium cations chemically bonded to sulfate ions and one zwitter ion are present in the structure of TGS. Carboxyl groups, amino groups, and sulfate ions are connected to each other in the crystal by a complex network of hydrogen bonds [2] (Fig. 1).

Since the mechanism of spontaneous polarization in TGS is related to the ordering of protons involved in the formation of hydrogen bonds [3],

the role of the state of aqueous or aqueous alcoholic solution (AAS) of TGS during crystal growth from this solution cannot be overestimated. In particular, it has been previously shown that the amount of water and its structural localization in the crystal at low and high temperatures differ. TGS crystals grown at room temperature (20°C) contain about 9 wt % of water, whereas when growing the crystal at temperatures below 0°C, the water content reaches almost 19 wt %. Most of the water is located in microinclusions rather than in the form of solid solution [1, 4–5].

The technological processing (TP) of solutions of various substances includes multiple consecutive dilutions accompanied by intensive vibration treatment. It can lead to changes in various physicochemical properties of TP substances. A large number of dilution steps leads to a theoretical reduction of the concentration of the initial substance in the solution of at least 10^{24} (i.e., the resulting solution may contain only single molecules of the dissolved

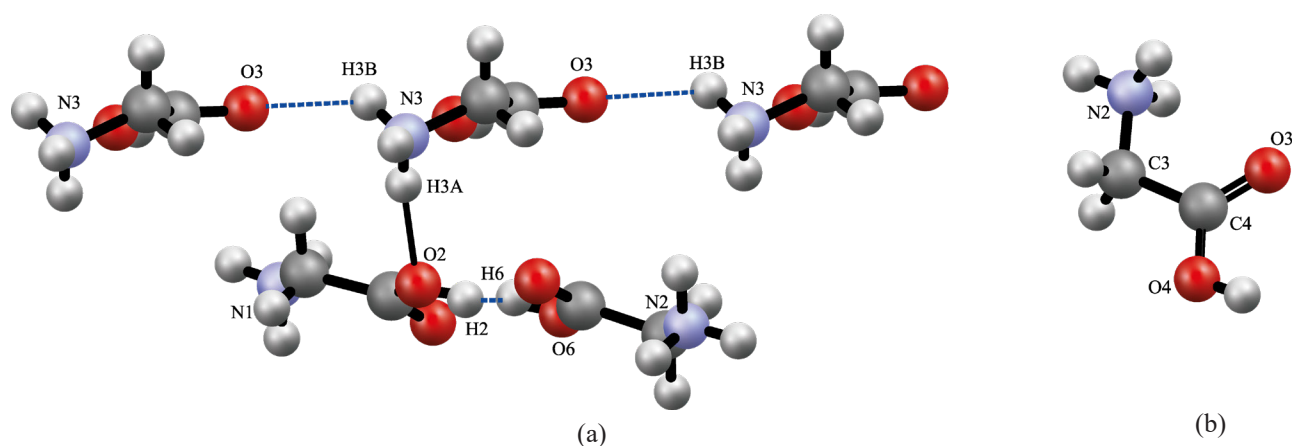


Fig. 1. Glycine groups and intermolecular hydrogen bonds (represented by lines-dots) in the TGS molecule (a) and a schematic representation of the glycine cation (b).

Structurally equivalent atoms are indicated by the same numbers.

Figures are created in Mercury soft (Cambridge Crystallographic Data Center, United Kingdom).

substance or not contain them at all). Despite this, such a solution differs in its physicochemical characteristics from the characteristics of the solvent: water or AAS [7–13]. A change in the nature of hydrogen bonds between water molecules in the substance, which has undergone this treatment, is also shown in comparison to usual water [13–20].

It was shown at the example of TP-antibodies (TP-Abs) to interferon-gamma (IFN- γ), that their biological effects are based on the modifying action of TP-Abs on its target [6, 21]. This is attained through the influence on the hydrate shells surrounding the protein in aqueous solution [22]. Thus, since TP affects the solution properties by changing the hydrogen bonds, which in turn are involved in the occurrence of spontaneous polarization in TGS, it can be assumed that the TP solution will also affect the structure of the crystal grown in such an aqueous solution, whose new properties may be fundamental for the realization of the effect.

The aim of this work is to study the structural features of TGS crystals grown using AAS of TP-Abs to IFN- γ in comparison with those of crystals grown using the technologically treated phosphate-buffered saline (PBS) or intact AAS. The study was carried out by X-ray diffraction (XRD) assay and Raman spectroscopy.

MATERIALS AND METHODS

Solvents for crystal preparation

In the process of crystal growth, the following types of aqueous alcoholic solvents for preparations of the parent solutions were used:

1) AAS of Abs to IFN- γ subjected to the process of gradual reduction of their initial concentration—TP-Abs to IFN- γ . The technique of obtaining of the TP-Abs to IFN- γ is as follows: the preparation of Abs to IFN- γ solution (2.5 mg/mL) was mixed with aqueous solution of ethyl alcohol (36 vol %) in a ratio of 1:100 with intensive vibration treatment to obtain the first centesimal dilution. All the subsequent dilutions contained one part of the previous solution and 99 parts of AAS, and intensive vibration treatment was applied at each subsequent dilution stage. Finally, the sample obtained was a mixture of centesimal dilutions: 12th, 30th, and 50th. More detailed description of the TP-Abs to IFN- γ preparation technique can be found in [7].

Based on the overall dilution ratio, the theoretical concentration of Ab in the final solution should not exceed $2.5 \cdot 10^{-24}$ mg/mL. However, according to physicochemical studies, for samples made with use of the high dilution preparation technique, this estimate may be incorrect due to the non-linear decrease in the concentration of the dissolved substance. In fact, it was shown that even at dilutions lower than 10^{24} -fold, the dissolved substance molecules can be retained due to the flotation effect [23, 24]. Abs to IFN- γ were produced in accordance with the current European Union Good Manufacturing Practice (GMP) requirements for starting materials¹ by *AB Biotechnology* (Edinburgh, United Kingdom).

¹ Europea U. Directive 2004/27/EC of the European Parliament and of the Council of March 31, 2004 Amending Directive 2001/83/EC on the Community Code Relating to Medicinal Products for Human Use. Official Journal of the European Union. L2004;136:34–57. URL: <https://eur-lex.europa.eu/legal-content/EN/TXT/PDF/?uri=CELEX:32004L0027>. Accessed November 01, 2023.

2) Placebo control solution in AAS was prepared using a similar dilution procedure applied to the PBS solution prepared from PBS tablet (*Sigma-Aldrich*, USA), pH = 7.2.

3) Intact control solution was an AAS, not subjected to any additional treatment.

All the solutions were prepared using water obtained with the Milli-Q purification system (*Millipore*, Darmstadt, Germany) and checked for possible impurities by fluorescence spectroscopy and specific conductivity measurements. The sample manufacturer is GMP certified, in order to ensure strict adherence to sample preparation protocols. All samples were prepared under clean conditions (purity class D) in a laminar flow hood using sterile automatic pipettes with sterile tips. All the samples were prepared on the same day by the same staff member and under the same conditions. The preparation protocol took into account any contamination of vials from other glassware, solvent batches or the atmosphere. This allowed compensation for the possible effects of variations in atmospheric pressure and temperature.

TGS crystal growth

Crystalline samples of TGS were grown from solutions using the above solvents by the method of gradual temperature reduction. The growth experiments were carried out in two stages. In the first stage, seed crystals (up to 3 mm in size) were prepared by spontaneous crystallization in a laboratory glass with the natural temperature reduction. Further, in order to obtain larger crystalline samples using the seed crystals, a controlled reduction in the temperature of the parent solution was carried out in a special laboratory programmable crystallization unit (crystallizer). The description of this crystallizer can be found in [25].

Preparation of the seed crystals

At the beginning, parent solutions were prepared in the crystallizer using the above solvents containing TP-Abs to IFN- γ , TP-PBS, and AAS with a concentration of 42 wt % TGS. Such solutions had a saturation temperature of about 40–45°C, determined by preheating the solution to temperatures slightly higher than the saturation temperature. Such overheating was performed, in order to prevent spontaneous crystallization of the solution during its pouring into the crystallizer [25].

For the preparation of the parent solutions, we used TGS of pure grade (*Shostka Chemical Reagents Plant*, Ukraine), which underwent additional purification. Additional purification consisted in fractional recrystallization in two stages. At the first stage, a saturated hot solution (prepared using

tridistilled water) was fabricated and then filtered from the precipitate on a Schott filter No. 3. This step was followed by spontaneous mass crystallization overnight with stirring. In the next step, the crystalline precipitate obtained was again dissolved in tridistilled water and the above procedure of the filtration and mass crystallization was repeated. Three parent solutions of 350 mL each were prepared.

A 50-mL aliquot was taken from each parent solution at a temperature higher than the saturation temperature and transferred to a separate laboratory glass. Here it was spontaneously crystallized for 8 h at a natural temperature reduction to room temperature (20°C) without stirring. After the aliquot cooled down, the remained solution was decanted from the formed seed crystals.

Preparation of crystals for research

Seed crystals were placed in the parent solution prepared in the crystallizer at the above-mentioned saturation temperature. Then the crystallizer was sealed. After 72 h of holding the parent solution with the inoculum crystal at saturation temperature, stirring was initiated at the temperature decrease. The temperature reduction was carried out for 14 days according to a special schedule (the temperature reduction rate was gradually increased from about 0.1°C/day in the 1st day to 4°C/day in the 14th day of cooling, similar to [26]). After that, the crystallizer was opened, the parent solution was decanted from the crystals. Then the crystals were removed from the crystallizer, blotted on filter paper and air-dried.

The grown crystals had a pronounced natural cut. After they had been obtained, the crystal samples were stored in plastic tubes at room temperature. From the parent solution with TP-Abs to IFN- γ , 4 large SST crystals (with a size in one direction of more than 5 mm) were grown. From the parent solution with TP-PBS, 5 large SST crystals (more than 5 mm) and 5 small crystals (less than 5 mm) were grown. From the parent solution with AAS, about 20 small crystals (less than 3 mm) were grown.

Preparation of crystals for XRD

For each type of solvent three crystal samples were investigated by XRD. The preparation of samples for XRD was carried out by splintering from the main crystal a fragment with the size not less than $0.1 \times 0.1 \times 0.1$ mm³. The visually perfect transparent crystal fragment selected with the help of an optical microscope was attached to a glass thread with the help of vacuum grease (Fig. 2).



Fig. 2. Photos of TGS crystals pasted on a glass thread for conducting XRD.

In order to determine the quality of the sample, a preliminary express scan was performed using the built-in function included in the CrysAlisPro XRD experiment control software package (*Rigaku*, USA)².

XRD

A Xcalibur, Sapphire 3, Gemini single crystal diffractometer (*Rigaku*, Japan), MoK_α radiation ($\lambda = 0.71073 \text{ \AA}$) was used for XRD studies. In the

experiment, ω -scanning with a step of 1° was used. The exposure was 15 s per step. The angular position of the CCD detector (54.25°) was chosen to record the reflections with the best resolution of $\sin\theta/\lambda \approx 0.5 \text{ \AA}^{-1}$.

The processing of diffractograms (peak search, determination of unit cell parameters, integration of reflections intensities) was carried out in automatic mode in the CrysAlisPro program (*Rigaku*, USA). The solution and refinement of the atomic structure of crystals was performed in the Shelx program complex using the ShelxLe graphical shell (*Shelx*, Germany)³.

² <https://www.rigaku.com/products/crystallography/crystalis>. Accessed November 01, 2023.

³ <https://www.shelxle.org/shelx/eingabe.php>. Accessed November 01, 2023.

Methodology for the determination of hydrogen atoms

Under normal conditions, TGS crystals are in the ferroelectric phase (Curie point (T_c) is 49°C). This ensures that the crystal is partitioned into domains possessing spontaneous polarization. Without additional measures (e.g., imposition of an external electric field), which are not available for the instrument configuration used, the XRD results of such material may contain artifacts related to twinning. Therefore, the position of only certain hydrogen atoms in the structure was determined from electron density difference synthesis. The missing hydrogen atoms were then added on the basis of geometric calculations of characteristic valence angles in organic compounds. However, in the final solution of each structure, all hydrogen atoms were localized and refined according to the so-called riding model to avoid fluctuations. The N–H, O–H, and C–H bond lengths, as well as valence angles and thermal parameters, were fixed. The exact coordinates are refined parameters and are calculated according to the standard scheme. The above approach is generally accepted and enabled us to avoid problems with the occurrence of distortions which contradict the fundamental crystallochemical approaches (e.g., unrealistically short or unrealistically long bonds between atoms) [3].

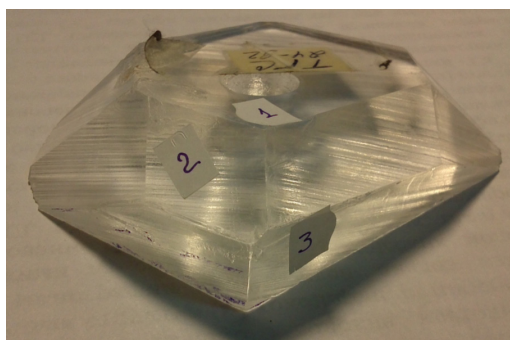
Raman spectroscopy

The Raman spectra of crystals were measured using an Integra Spectra micro-Raman spectrometer

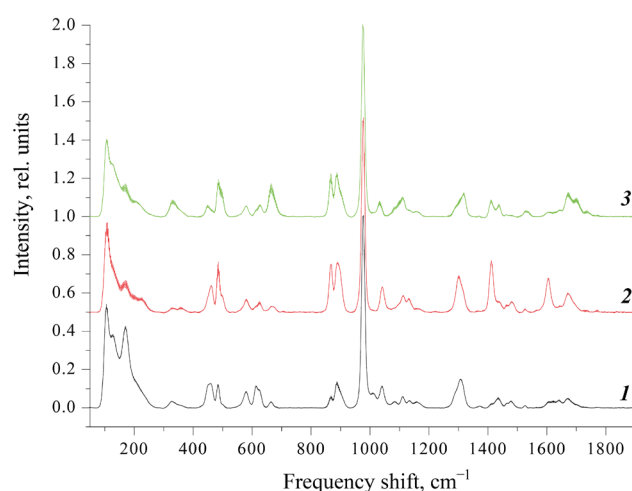
(*NT-MDT*, Zelenograd, Russia). The crystal was placed on a cover glass and positioned on the slide of an inverted microscope, in order that the trial laser beam (MSL-III-532 50 mW laser, *Changchun New Industries Optoelectronics Technology Co.*, China) fell on the selected facets. Measurement parameters: excitation light wavelength 532 nm, power on the sample approximately 5 mW, grating 600, objective lens 5×, recording time of one spectrum 60 s.

Four crystals grown from a parent solution containing TP-Abs to IFN- γ and two crystals grown from a parent solution containing TP-PBS were analyzed. Three natural facets of each crystal were analyzed. Three spectra were measured from each facet while moving the crystal slightly across the slide.

In addition, the facet spectra of a reference TGS crystal (Fig. 3a), previously grown using the technique described in [26], were measured. The TGS reference crystal under consideration belongs to the monoclinic syngony with the $2/m$ point group. This point group is characterized by open simple shapes: pinocoids and rhombic prisms. The measured spectra of different faces of the reference crystal are shown in Fig. 3b. The crystal faces were conventionally labeled as type *1*, *2*, or *3* depending on the shape of the spectrum. Based on the data of [26] with the description of the basic equilibrium faceting of the TGS crystal, we can refer *1*, *2*, and *3* type faces to the following simple forms. By shape and location, the facet of type *1* (as well as by the trace from the



(a)



(b)

Fig. 3. Standard crystal of TGS (a) and the RAMAN spectra from the characteristic facets of this crystal (b).

The numbers indicate the facets from which the corresponding spectra were recorded.

All Raman spectra are presented here and further as average value \pm error of the average.

columnar seed holder) belongs to the pinocoid facet belonging to the $\{001\}$ family. The face of type 2 belongs to the family of faces of the rhombic prism $\{-111\}$. The facet of type 3 (neighboring between facets a and b with indices (100) and (010), respectively) belongs to the faces of the rhombic prism $\{110\}$.

The faces of the crystals investigated (grown from the parent solution containing TP-Abs to IFN- γ or TP-PBS) were correlated with the faces of the reference TGS crystal on the basis of the correspondence of Raman spectra. For this purpose, the ratio of spectral bands in the regions of 860–930, 1060–1140, 1360–1440, and 1560–1700 cm^{-1} was visually evaluated. Comparison of the investigated crystals of TGS was carried out on the basis of the spectra of those faces which correspond to the spectra of the face of type 2 (family of faces of rhombic prism $\{-111\}$) of the standard crystal of TGS.

When processing the measured spectra, we subtracted the background value obtained by fitting the baseline with a polynomial function coinciding with the points of the spectrum minimum. Then the spectra obtained were normalized by the intensity of the band with frequency $\nu = 975 \text{ cm}^{-1}$ (the most intense band of the spectrum due to vibrations of the SO_4 group). After that, we determined the intensity of peaks with $\nu = 1671 \text{ cm}^{-1}$ and 1604 cm^{-1} .

The intensities of maxima on the spectra obtained from one face of one crystal were averaged. The mean value and the error of the mean at each point characterizing the statistical scatter of the data were given.

Statistical analysis

Analysis and visualization of the data obtained were performed using the R statistical computing environment version 4.0.2 (*R Foundation for Statistical Computing*, Vienna, Austria).

Descriptive statistics were calculated based on the results of Raman spectroscopy, while comparison of groups was performed using Student's t -test. Distribution normality was evaluated by the Shapiro–Wilk test, while homogeneity of dispersions was evaluated by the Bartlett test. XRD data were compared using the parametric Tukey's criterion.

Differences between the analyzed groups were considered statistically significant with an error probability $p < 0.05$ (i.e., the probability of obtaining such or stronger differences, provided that there were no differences between the compared groups, was less than 5%).

RESULTS AND DISCUSSION

XRD

According to XRD data, all crystals possessed symmetry corresponding to the space group $P2_1$ of the monoclinic syngony, i.e., they did not contain an inversion center. In all experiments, the value of the signal-to-noise ratio $(\Delta/\sigma)_{\text{max}}/(\Delta/\sigma)_{\text{av}}$ was close or strictly equal to zero. This indicates that these models meet the real minimum of the least squares method, i.e., the model of atomic-molecular composition of crystals had been chosen correctly. The high quality of the crystal and the correspondence of the found model to the experimental data are evidenced by the following values:

- The maximum value of the scattering angles θ exceeds 36° , indicating a good intensity of reflection by crystals at far scattering angles. It also corresponds to the high number of measured reflection intensities (more than 12000).
- The minimum and maximum residual electron density in most experiments does not exceed the absolute value of $0.5 \text{ e}/\text{A}^3$, corresponding to a high degree of fit of the model to the experimental data.
- All calculated R-factors (inconsistency factors) are quite small, also corresponding to a high degree of model fit to the experimental data.

The structure of TGS is complex and represents a grid of $\text{NH}_2\text{CH}_2\text{COOH}$ glycine molecules and SO_4 tetrahedrons linked by O–H...O and N–H...O hydrogen bonds (Fig. 1). The lengths of valence bonds (Table 1), as well as valence angles (Table 2), were calculated from the XRD data for the grown TGS samples.

The statistical analysis of the obtained results revealed statistically significant differences in the values of N2–C3 bond length between the samples of TGS grown from solutions containing TP-Abs to IFN- γ and TP-PBS (Fig. 4).

This parameter corresponds to the distance between the amino group $-\text{NH}_2$ and the methylene bridge $-\text{CH}_2-$ of the glycine molecule. The nearest environment of the $-\text{NH}_2$ functional group, which is not connected with it by a rigid covalent bond, is represented by two SO_4^{2-} anions and a similar grouping of the neighboring glycine molecule. Since these groupings of atoms include electronegative elements (O, N) and electropositive hydrogen, all the conditions for the formation of hydrogen bonds between these groupings are met. The observed difference in the lengths of N2–C3 bonds can be explained by differences in the proton occupancy of the positions of hydrogen bonds, in which the N2 atoms participate.

Table 1. Lengths of interatomic bonds in TGS crystals grown from various parent solutions, Å (measurement errors are given in parentheses)

Bond	TP-Abs to IFN- γ			TP-PBS			AAS		
	1	2	3	1	2	3	1	2	3
C1–N1	1.466(4)	1.466(3)	1.465(3)	1.465(3)	1.476(7)	1.470(3)	1.467(3)	1.472(4)	1.467(3)
C1–C2	1.503(4)	1.507(3)	1.504(3)	1.504(3)	1.512(8)	1.505(3)	1.500(3)	1.500(4)	1.505(3)
S1–O9	1.4647(13)	1.4664(9)	1.4654(10)	1.4652(10)	1.464(2)	1.4651(9)	1.4602(10)	1.4665(11)	1.4668(10)
S1–O8	1.466(2)	1.4674(15)	1.4668(18)	1.4681(16)	1.468(3)	1.4670(15)	1.4637(15)	1.4683(19)	1.4690(17)
S1–O10	1.4765(19)	1.4794(14)	1.4800(17)	1.4773(16)	1.477(3)	1.4777(15)	1.4732(14)	1.4775(18)	1.4788(17)
C3–C4	1.512(4)	1.514(3)	1.513(3)	1.511(3)	1.500(8)	1.514(3)	1.510(3)	1.518(4)	1.513(3)
N3–C5	1.466(3)	1.470(2)	1.470(3)	1.470(3)	1.473(6)	1.470(3)	1.465(3)	1.470(3)	1.470(3)
C6–O5	1.201(3)	1.205(2)	1.201(2)	1.202(2)	1.202(5)	1.201(2)	1.197(2)	1.205(2)	1.206(2)
C6–O6	1.303(2)	1.3026(18)	1.304(2)	1.304(2)	1.298(4)	1.302(2)	1.3013(19)	1.303(2)	1.302(2)
C6–C5	1.511(3)	1.5102(19)	1.512(2)	1.511(2)	1.509(4)	1.515(2)	1.508(2)	1.512(2)	1.514(2)
S1–O7	1.4833(13)	1.4847(9)	1.4838(11)	1.4832(10)	1.484(2)	1.4840(10)	1.4799(10)	1.4852(11)	1.4864(11)
O1–C2	1.230(4)	1.229(3)	1.231(3)	1.232(3)	1.218(7)	1.229(3)	1.229(3)	1.234(3)	1.229(3)
O2–C2	1.284(4)	1.287(2)	1.285(3)	1.286(3)	1.280(6)	1.286(3)	1.282(3)	1.285(3)	1.285(3)
N2–C3	1.470(4)	1.468(3)	1.467(3)	1.466(3)	1.460(7)	1.461(3)	1.461(3)	1.463(4)	1.467(3)
O3–C4	1.209(4)	1.216(3)	1.216(3)	1.212(3)	1.223(7)	1.216(3)	1.209(3)	1.212(3)	1.216(3)

Table 2. Values of valence bond angles in TGS crystals grown from various parent solutions, degrees (measurement errors are given in parentheses)

Angle	TP-Abs to IFN- γ			TP-PBS			AAS		
	1	2	3	1	2	3	1	2	3
N1–C1–C2	111.4(3)	111.42(17)	111.6(2)	111.5(2)	110.9(5)	111.31(18)	111.25(18)	111.3(2)	111.5(2)
O9–S1–O8	111.01(15)	111.28(11)	111.15(12)	111.12(12)	111.0(3)	111.13(11)	111.27(11)	111.10(13)	111.12(12)
O9–S1–O10	110.22(15)	110.06(11)	110.21(13)	110.27(12)	110.5(3)	110.30(11)	110.19(11)	110.29(13)	110.18(12)
O8–S1–O10	109.72(8)	109.78(6)	109.70(7)	109.65(7)	109.68(12)	109.72(6)	109.59(6)	109.74(7)	109.81(7)
O9–S1–O7	110.26(8)	110.24(6)	110.27(7)	110.29(7)	110.27(12)	110.25(6)	110.26(6)	110.21(7)	110.29(6)
O8–S1–O7	108.11(14)	108.02(10)	108.07(12)	108.00(11)	107.8(2)	107.99(10)	108.09(10)	108.11(13)	108.00(12)
O10–S1–O7	107.43(14)	107.35(10)	107.34(12)	107.41(12)	107.5(3)	107.36(11)	107.35(10)	107.30(13)	107.35(12)

Table 2. Continued

Bond	TP-Abs to IFN- γ			TP-PBS			AAS		
	1	2	3	1	2	3	1	2	3
O1–C2–O2	126.2(3)	126.12(19)	126.2(2)	126.1(2)	127.1(6)	126.2(2)	126.1(2)	125.7(3)	126.2(2)
O1–C2–C1	120.4(2)	120.49(17)	120.5(2)	120.52(19)	120.6(4)	120.68(18)	120.62(17)	120.8(2)	120.5(2)
O2–C2–C1	113.4(3)	113.40(19)	113.3(2)	113.3(2)	112.3(5)	113.1(2)	113.2(2)	113.5(2)	113.3(2)
N2–C3–C4	110.8(3)	110.79(16)	111.0(2)	110.8(2)	111.7(5)	111.01(18)	110.81(18)	111.1(2)	111.0(2)
O5–C6–O6	125.2(2)	125.10(14)	125.04(17)	125.09(16)	125.3(3)	125.19(15)	124.99(15)	124.99(17)	125.07(16)
O5–C6–C5	121.6(2)	121.59(14)	121.71(17)	121.76(16)	121.2(3)	121.64(16)	121.72(15)	121.62(17)	121.51(16)
O6–C6–C5	113.24(17)	113.30(12)	113.25(15)	113.14(14)	113.4(3)	113.17(13)	113.28(13)	113.39(15)	113.43(14)
N3–C5–C6	112.17(18)	111.84(13)	111.92(15)	111.97(14)	111.8(3)	111.80(14)	111.87(13)	111.88(16)	111.85(15)
O3–C4–O4	126.2(3)	126.5(2)	126.2(2)	126.1(2)	125.0(6)	126.2(2)	126.3(2)	126.6(3)	126.2(2)
O3–C4–C3	122.2(3)	121.81(17)	121.8(2)	122.1(2)	122.1(5)	121.77(19)	121.98(18)	121.7(2)	121.9(2)
O4–C4–C3	111.5(3)	111.71(19)	111.9(2)	111.8(2)	112.8(5)	112.0(2)	111.7(2)	111.6(3)	111.9(2)

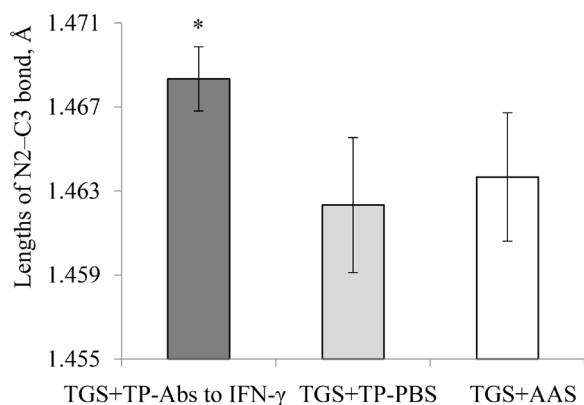


Fig. 4. Average value of the N2–C3 valence bond lengths for TGS crystals grown from a solution containing TP-Abs to IFN- γ , as well as from control solutions (Mean \pm Standard deviation (M \pm Sd)).

* $p < 0.05$ relative to the intensity for TGS crystals from a solution containing the TP-PBS.

Raman spectroscopy

The measured results of the Raman spectra of crystals obtained from solutions containing TP-Abs to IFN- γ and TP-PBS are presented in Table 3. The Raman spectra for each type of crystals are shown in Fig. 5. The spectra presented in Fig. 5a

correspond to the shape (namely, the ratio of spectral bands in the regions 860–930, 1060–1140, 1360–1440, and 1560–1700 cm^{-1}) of the spectrum of the face of the reference TGS crystal, conventionally labeled **2** (Fig. 3b). The intensity of the peak at 1671 cm^{-1} differs in crystals of different types (Fig. 5b). Therefore, we further compared the intensities of this maximum using statistical methods.

Statistical analysis using the Mann–Whitney criterion showed that band intensity at 1671 cm^{-1} for the samples obtained in the presence of TP-Abs to IFN- γ was statistically significantly higher than the intensity of the band of the same name for the samples grown in the presence of TP-PBS ($p < 0.05$) (Fig. 5c). The vibrational mode at 1671 cm^{-1} in the Raman spectra of TGS crystals corresponds to the valence vibrations of the C=O group (stretching-compression vibrations) [27]. These groups of atoms are involved in hydrogen bonding of individual glycine molecules into chains. Glycine group G3 is known to be ordered into chains by means of N3–H3B...O3 bonds, and glycine groups G1 and G2 form dimers by means of O2–H2...H4–O4 bonds [28]. More active binding of glycine molecules, with a degree of hydrogen bond occupancy by protons close to unity at a given position, leads to decreased intensity of valence

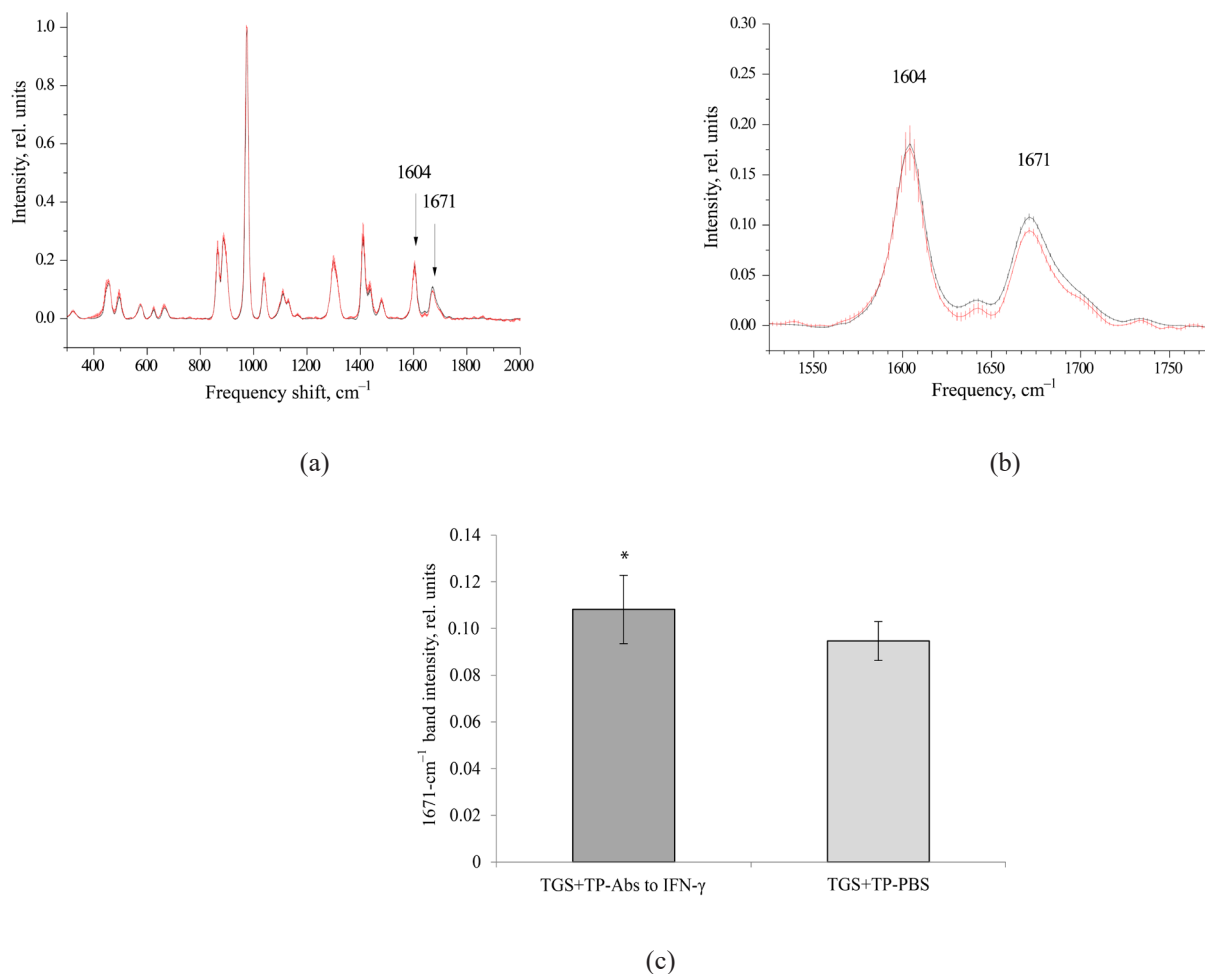


Fig. 5. (a) RAMAN spectra obtained from the type 2 facet of crystals grown in the presence of TP-Abs to IFN- γ (black line) and TP-PBS (red line). (b) Spectral region on a larger scale. (c) Intensity of the Raman band with $\nu = 1671 \text{ cm}^{-1}$ for TGS crystals grown from a solution containing TP-Abs to IFN- γ ($M \pm Sd$); * $p < 0.05$ relative to the intensity for TGS crystals from a solution containing the TP-PBS.

vibrations of the C=O double bond. It also leads to a decrease in the intensity of the corresponding vibrational mode of the Raman spectrum. Accordingly, with a decrease in the degree of occupancy of hydrogen bond positions in glycine dimers and chains, an increase in the intensity of the vibrational mode at 1671 cm^{-1} is observed. Thus, this parameter allows us to indirectly make a comparison between groups of samples of TGS crystals by the degree of occupancy of hydrogen bond positions. In this case it is probable that differences in the intensity of vibrations and polarizability can be caused by a small change in the microenvironment of these bonds in the glycine molecule. The stabilization of the zwitter-ion conformer most likely occurs with the participation of one water molecule [29].

Thus, the results of crystal studies by Raman spectroscopy show that a smaller number of hydrogen bonds is formed in the sample of TGS crystal obtained in the presence of TP-Abs to IFN- γ .

According to the XRD data, we can observe a change in the length of the N2–C3 bond within one molecule. TGS crystals are known to manifest a proton hopping mechanism of proton transfer along the OH–O hydrogen bonding network [30]. The differences in the degree of proton occupancy of hydrogen bond positions can account for the observed difference in the lengths of N2–C3 bonds. In the crystal grown in the presence of TP-Abs to IFN- γ , this bond appears to be longer than in crystals grown from control solutions (TP-PBS and AAS). This implies a decrease in the number of hydrogen bonds. This conclusion is supported by the results obtained in the studies by Raman spectroscopy.

Summarizing the data obtained, we can conclude that both methods show that a smaller number of hydrogen bonds is formed in the sample of TGS crystal when obtained in the presence of TP-Abs to IFN- γ , when compared to crystals grown from control solutions (TP-PBS and AAS). The action

Table 3. Intensity of characteristic bands at 1671 and 1604 cm⁻¹

Band intensity at 1671 cm ⁻¹		Band intensity at 1604 cm ⁻¹	
TGS crystals obtained from a solution containing TP-Abs to IFN- γ	TGS crystals obtained from a solution containing TP-PBS	TGS crystals obtained from a solution containing TP-Abs to IFN- γ	TGS crystals obtained from a solution containing TP-PBS
0.11095	0.08676	0.17695	0.10601
0.12549	0.08759	0.22240	0.09830
0.10790	0.09273	0.17639	0.10012
0.11084	0.10294	0.14632	0.20799
0.07034	0.11127	0.08469	0.24110
0.11334	0.09324	0.13901	0.22482
0.10890	0.08996	0.13426	0.21202
0.13704	0.09287	0.28414	0.22250
0.12293	–	0.25905	–
0.12321	–	0.25545	–
0.12234	–	0.22994	–
0.12176	–	0.22812	–
0.11706	–	0.22272	–
0.09194	–	0.17393	–
0.10321	–	0.11153	–
0.09831	–	0.18336	–
0.09902	–	0.17805	–
0.10156	–	0.17666	–
0.09457	–	0.17712	–
0.10626	–	0.14743	–
0.09664	–	0.14155	–
0.09604	–	0.13451	–

of TP-Abs to IFN- γ , not directed on its target, is probably due to the influence on the growth of TGS of the aqueous solution which acquired new properties when compared to control solutions in the process

of technological processing. This corresponds to the previously obtained data on the realization of the effect of technologically processed proteins through the influence on the hydrate shells of the target molecule [22].

CONCLUSIONS

Summarizing the experimental results, we can conclude that the main effect of TP-Abs solution used to grow the TGS crystals on the properties of these crystals consists in changing the properties of the proton sub-lattice of the crystal. This is a structural component of the crystal, which is the most sensitive to the effects of external factors. The significant importance of water in the electrical properties of crystals has been shown earlier. Therefore, it will be of further interest to study not only the structure but also the properties of crystals grown from AAS subjected to various types of technological processing.

Acknowledgments

The work was financially supported by *Materia Medica Holding, Moscow, Russia*.

Authors' contributions

G.O. Stepanov – data analysis, conceptualization, writing the text of the initial draft;

N.N. Rodionova – data analysis, conceptualization, writing the text of the initial draft;

R.R. Konstantinov – data analysis, editing the article;

K.A. Subbotin – counseling, editing the article.

Conflict of interest

The authors declared the following potential conflicts of interest in connection with the authorship and/or publication of this article: G.O. Stepanov, N.N. Rodionova, and R.R. Konstantinov are employees of *Materia Medica Holding*. *Materia Medica Holding* decided to publish the work and covered the costs associated with the publication of the article, paid for the experimental work, participated in the writing of the manuscript.

REFERENCES

1. Yacenko O.B., Chudotvortsev I.G., Stekhanova G.D., Milovidova S.D., Rogazinskaya O.V. Density and contents of water in triglycinesulfate crystals. *Vestnik Voronezhskogo gosudarstvennogo universiteta. Seriya: Khimiya. Biologiya. Farmatsiya = Proceedings of Voronezh State University. Series: Chemistry. Biology. Pharmacy*. 2006;(2):117–121 (in Russ.).
2. Epifanov G.I. *Fizika tverdogo tela (Solid State Physics)*. Moscow: Vysshaya shkola; 1977. 288 p. (in Russ.).
3. Lines M., Glass A. *Segnetoelektriki i rodstvennye im materialy (Ferroelectrics and Related Materials)*. Transl. from. Engl. Moscow: Mir; 1981. 736 p. (in Russ.).
[Lines M.E., Glass A.M. *Principles and Application of Ferroelectrics and Related Materials*. Oxford: Clarendon Press; 1977. 680 p.]
4. Stekhanova Zh.D., Yatsenko O.B., Milovidova S.D., Sidorkin A.S., Rogazinskaya O.V., Yur'ev A.N. Dielectric properties of crystals triglycine sulfate, grown from aqueous solutions at the temperatures below 0°C. *Vestnik Voronezhskogo gosudarstvennogo universiteta. Seriya: Khimiya. Biologiya. Farmatsiya = Proceedings of Voronezh State University. Series: Chemistry. Biology. Pharmacy*. 2004;(2):46–49 (in Russ.).
5. Stekhanova Z.D., Yatsenko O.B., Milovidova S.D., et al. Properties of Triglycine Sulfate Crystals Grown from Aqueous Solutions. *Russ. J. Appl. Chem*. 2005;78(1):42–49. <https://doi.org/10.1007/s11167-005-0228-9>

СПИСОК ЛИТЕРАТУРЫ

1. Яценко О.Б., Чудотворцев И.Г., Стеханова Ж.Д., Миловидова С.Д., Рогазинская О.В. Плотность и содержание воды в кристаллах триглицинсульфата. *Вестник ВГУ. Серия: Химия. Биология. Фармация*. 2006;(2):117–121.
2. Епифанов Г.И. *Физика твердого тела*. М.: Высшая школа; 1977. 288 с.
3. Лайнс М., Гласс А. *Сегнетоэлектрики и родственные им материалы*: пер. с англ. М.: Мир; 1981. 736 с.
4. Стеханова Ж.Д., Яценко О.Б., Миловидова С.Д., Сидоркин А.С., Рогазинская О.В., Юрьев А.Н. Диэлектрические свойства кристаллов триглицинсульфата, выращенных из водных растворов при температурах ниже 0°C. *Вестник ВГУ. Серия: Химия. Биология. Фармация*. 2004;(2):46–49.
5. Стеханова Ж.Д., Яценко О.Б., Миловидова С.Д., Сидоркин А.С., Рогазинская О.В. Свойства кристаллов триглицинсульфата, выращенных из водных растворов. *Журн. прикладной химии*. 2005;78(1):45–51.
6. Epstein O. The spatial homeostasis hypothesis. *Symmetry*. 2018;10(4):103. <https://doi.org/10.3390/sym10040103>
7. Рыжкина И.С., Муртазина Л.И., Киселева Ю.В., Коновалов А.И. Самоорганизация и физико-химические свойства водных растворов антител к интерферону-гамма в сверхвысоком разведении. *Доклады Академии наук*. 2015;462(2):185–189. <https://doi.org/10.7868/S0869565215140170>

[Original Russian Text: Stekhanova Z.D., Yatsenko O.B., Milovidova S.D., Sidorkin A.S., Rogazinskaya O.V. Properties of Triglycine Sulfate Crystals Grown from Aqueous Solutions. *Zhurnal Prikladnoi Khimii*. 2005;78(1):45–51 (in Russ.).]

6. Epstein O. The spatial homeostasis hypothesis. *Symmetry*. 2018;10(4):103. <https://doi.org/10.3390/sym10040103>

7. Ryzhkina I.S., Murtazina L.I., Kiseleva Ju.V., et al. Self-organization and physicochemical properties of aqueous solutions of the antibodies to interferon gamma at ultrahigh dilution. *Dokl. Phys. Chem.* 2015;462(1):110–114. <https://doi.org/10.1134/S0012501615050048>

[Original Russian Text: Ryzhkina I.S., Murtazina L.I., Kiseleva Ju.V., Kononov A.I. Self-organization and physicochemical properties of aqueous solutions of the antibodies to interferon gamma at ultrahigh dilution. *Doklady Akademii Nauk*. 2015;462(2):185–189 (in Russ.). <https://doi.org/10.7868/S0869565215140170>]

8. Ryzhkina I., Murtazina L., Gainutdinov K., Kononov A. Diluted aqueous dispersed systems of 4-aminopyridine: The relationship of self-organization, physicochemical properties, and influence on the electrical characteristics of neurons. *Front. Chem.* 2021;9:623860. <https://doi.org/10.3389/fchem.2021.623860>

9. Kononov A.I., Mal'tseva E.L., Ryzhkina I.S., et al. Formation of nanoassociates is a factor determining physicochemical and biological properties of highly diluted aqueous solutions. *Dokl. Phys. Chem.* 2014;456(2):86–89. <https://doi.org/10.1134/S0012501614060050>

[Original Russian Text: Kononov A.I., Ryzhkina I.S., Murtazina L.I., Kiseleva Y.V., Mal'tseva E.L., Kasparov V.V., Pal'mina N.P. Formation of nanoassociates is a factor determining physicochemical and biological properties of highly diluted aqueous solutions. *Doklady Akademii Nauk*. 2014;456(5):561–564 (in Russ.). <https://doi.org/10.7868/S0869565214170174>]

10. Lobyshev V.I. Biological activity of solutions of substances at low and ultra low concentrations. *Biophysica*. 2022;67(4):523–533. <https://doi.org/10.1134/S0006350922040145>

[Original Russian Text: Lobyshev V.I. Biological activity of solutions of substances at low and ultra low concentrations. *Biofizika*. 2022;67(4):658–670 (in Russ.). <https://doi.org/10.31857/S0006302922040044>]

11. Lobyshev V.I. Dielectric characteristics of highly diluted aqueous diclofenac solutions in the frequency range of 20 Hz to 10 MHz. *Phys. Wave Phen.* 2019;27(2):119–127. <https://doi.org/10.3103/S1541308X19020067>

12. Lobyshev V.I. Evolution of high-frequency conductivity of pure water samples subjected to mechanical action: effect of a hypomagnetic field. *Phys. Wave Phen.* 2021;29(2):98–101. <https://doi.org/10.3103/S1541308X21020084>

13. Yablonskaya O., Buravleva E., Novikov K., Voeikov V. Peculiarities of the physicochemical properties of hydrated C60 fullerene solutions in a wide range of dilutions. *Front. Phys.* 2021;9:627265. <https://doi.org/10.3389/fphy.2021.627265>

14. Belov V.V., Belyaeva I.A., Shmatov G.P., et al. IR spectroscopy of thin water layers and the mechanism of action α -tocopherol in ultra low concentrations. *Dokl. Phys. Chem.* 2011;439(1):123–126. <https://doi.org/10.1134/S0012501611070013>

[Original Russian Text: Belov V.V., Belyaeva I.A., Shmatov G.P., Zubareva G.M., Pal'mina N.P. IR spectroscopy of thin water layers and the mechanism of action α -tocopherol in ultra low concentrations. *Doklady Akademii Nauk*. 2011;439(1):68–71 (in Russ.).]

8. Ryzhkina I., Murtazina L., Gainutdinov K., Kononov A. Diluted aqueous dispersed systems of 4-aminopyridine: The relationship of self-organization, physicochemical properties, and influence on the electrical characteristics of neurons. *Front. Chem.* 2021;9:623860. <https://doi.org/10.3389/fchem.2021.623860>

9. Коновалов А.И., Мальцева Е.Л., Рьзжкина И.С., Муртазина Л.И., Киселева Ю.В., Каспаров В.В., Пальмина Н.П. Образование наноассоциатов – фактор, определяющий физико-химические и биологические свойства высоко-разбавленных водных растворов. *Доклады Академии наук*. 2014;456(5):561–564. <https://doi.org/10.7868/S0869565214170174>

10. Лобышев В.И. Биологическая активность малых и сверхмалых концентраций. *Биофизика*. 2022;67(4):658–670. <https://doi.org/10.31857/S0006302922040044>

11. Lobyshev V.I. Dielectric characteristics of highly diluted aqueous diclofenac solutions in the frequency range of 20 Hz to 10 MHz. *Phys. Wave Phen.* 2019;27(2):119–127. <https://doi.org/10.3103/S1541308X19020067>

12. Lobyshev V.I. Evolution of high-frequency conductivity of pure water samples subjected to mechanical action: effect of a hypomagnetic field. *Phys. Wave Phen.* 2021;29(2):98–101. <https://doi.org/10.3103/S1541308X21020084>

13. Yablonskaya O., Buravleva E., Novikov K., Voeikov V. Peculiarities of the physicochemical properties of hydrated C60 fullerene solutions in a wide range of dilutions. *Front. Phys.* 2021;9:627265. <https://doi.org/10.3389/fphy.2021.627265>

14. Белов В.В., Беляева И.А., Шматов Г.П., Зубарева Г.М., Пальмина Н.П. ИК-спектроскопия тонких слоев воды и механизм действия α -токоферола в малых дозах. *Доклады Академии наук*. 2011;439(1):68–71.

15. Бревик И., Шаповалов А.В. Эффекты низкой концентрации в водных растворах в рамках фрактальной подхода. *Известия высших учебных заведений. Физика*. 2022;65(2):3–13. <https://doi.org/10.17223/00213411/65/2/3>

16. Shishkina A.V., Ksenofontov A.A., Penkov N.V., Vener M.V. Diclofenac ion hydration: experimental and theoretical search for anion pairs. *Molecules*. 2022;27(10):3350. <https://doi.org/10.3390/molecules27103350>

17. Slatinskaya O.V., Pyrkov Yu.N., Filatova S.A., Guryev D.A., Penkov N.V. Study of the effect of europium acetate on the intermolecular properties of water. *Front. Phys.* 2021;9:641110. <https://doi.org/10.3389/fphy.2021.641110>

18. Penkov N.V. Peculiarities of the perturbation of water structure by ions with various hydration in concentrated solutions of CaCl₂, CsCl, KBr, and KI. *Phys. Wave Phen.* 2019;27(2):128–134. <https://doi.org/10.3103/S1541308X19020079>

19. Penkov N., Fesenko E. Development of terahertz time-domain spectroscopy for properties analysis of highly diluted antibodies. *Appl. Sci.* 2020;10(21):7736. <https://doi.org/10.3390/app10217736>

20. Penkov N. Antibodies processed using high dilution technology distantly change structural properties of IFN γ aqueous solution. *Pharmaceutics*. 2021;13(11):1864. <https://doi.org/10.3390/pharmaceutics13111864>

21. Tarasov S.A., Gorbunov E.A., Don E.S., Emelyanova A.G., Kovalchuk A.L., Yanamala N., Schleker A.S.S., Klein-Seetharaman J., Groenestein R., Tafani J-P., van der Meide P., Epstein O.I. Insights into the mechanism of action of highly diluted biologics. *J. Immunol.* 2020;205(5):1345–1354. <https://doi.org/10.4049/jimmunol.2000098>

22. Woods K.N. Modeling of protein hydration dynamics is supported by THz spectroscopy of highly diluted solutions. *Front. Chem.* 2023;11:1131935. <https://doi.org/10.3389/fchem.2023.1131935>

15. Brevik I., Shapovalov A.V. Effects of low concentration in aqueous solutions within the fractal approach. *Russ. Phys. J.* 2022;65(2):197–207 (in Russ.). <https://doi.org/10.1007/s11182-022-02623-3>
- [Original Russian Text: Brevik I., Shapovalov A.V. Effects of low concentration in aqueous solutions within the fractal approach. *Izvestiya Vysshikh Uchebnykh Zavedenii. Fizika.* 2022;65(2):3–13 (in Russ.). <https://doi.org/10.17223/00213411/65/2/3>]
16. Shishkina A.V., Ksenofontov A.A., Penkov N.V., Vener M.V. Diclofenac ion hydration: experimental and theoretical search for anion pairs. *Molecules.* 2022;27(10):3350. <https://doi.org/10.3390/molecules27103350>
17. Slatinskaya O.V., Pyrkov Yu.N., Filatova S.A., Guryev D.A., Penkov N.V. Study of the effect of europium acetate on the intermolecular properties of water. *Front. Phys.* 2021;9:641110. <https://doi.org/10.3389/fphy.2021.641110>
18. Penkov N.V. Peculiarities of the perturbation of water structure by ions with various hydration in concentrated solutions of CaCl₂, CsCl, KBr, and KI. *Phys. Wave Phen.* 2019;27(2):128–134. <https://doi.org/10.3103/S1541308X19020079>
19. Penkov N., Fesenko E. Development of terahertz time-domain spectroscopy for properties analysis of highly diluted antibodies. *Appl. Sci.* 2020;10(21):7736. <https://doi.org/10.3390/app10217736>
20. Penkov N. Antibodies processed using high dilution technology distantly change structural properties of IFN γ aqueous solution. *Pharmaceutics.* 2021;13(11):1864. <https://doi.org/10.3390/pharmaceutics13111864>
21. Tarasov S.A., Gorbunov E.A., Don E.S., Emelyanova A.G., Kovalchuk A.L., Yanamala N., Schleker A.S.S., Klein-Seetharaman J., Groenestein R., Tafani J-P., van der Meide P., Epstein O.I. Insights into the mechanism of action of highly diluted biologics. *J. Immunol.* 2020;205(5):1345–1354. <https://doi.org/10.4049/jimmunol.2000098>
22. Woods K.N. Modeling of protein hydration dynamics is supported by THz spectroscopy of highly diluted solutions. *Front. Chem.* 2023;11:1131935. <https://doi.org/10.3389/fchem.2023.1131935>
23. Bunkin N.F., Shkirin A.V., Ninham B.W., Chirikov S.N., Chaikov L.L., Penkov N.V., Kozlov V.A., Gudkov S.V. Shaking-induced aggregation and flotation in immunoglobulin dispersions: differences between water and water-ethanol mixtures. *ACS Omega.* 2020;5(24):14689–14701. <https://doi.org/10.1021/acsomega.0c01444>
24. Chikramane P.S., Kalita D., Suresh A.K., Kane S.G., Bellare J.R. Why extreme dilutions reach non-zero asymptotes: a nanoparticulate hypothesis based on froth flotation. *Langmuir.* 2012;28(45):15864–15875. <https://doi.org/10.1021/la303477s>
25. Vainshtein B.K. *Sovremennaya kristallografiya: v 4 t. T. 3. Obrazovanie kristallov (Modern Crystallography: in 4 v. Vol. 3. Formation of Crystals).* Moscow: Nauka; 1980. 408 p. (in Russ.).
26. Koldobskaya M.F., Gavrilova I.V. Growing large faceted TGS crystals in laboratory conditions. In: *Rost kristallov (Crystal Growth).* Moscow: AN USSR; 1961. V. 3. P. 278–282 (in Russ.).
27. Malekfar R., Daraei A. Raman scattering and electrical properties of TGS:PCo (9%) crystal as ambient temperature IR detector. *Acta Physica Polonica A.* 2008;114(4):859–867. <http://doi.org/10.12693/APhysPolA.114.859>
28. Zheludev I.S. *Physics of Crystalline Dielectrics.* V. 1. *Crystallography and Spontaneous Polarization.* New York: Springer; 1971. 346 p. <https://doi.org/10.1007/978-1-4684-8076-4>
29. Крауклис И.В., Тулуб А.В., Головин А.В., Челибанов В.П. Спектры комбинационного рассеяния света глицина и их моделирование в дискретно-континуальной модели сольватной оболочки воды. *Оптика и спектроскопия.* 2020;128(10):1488–1491. <https://doi.org/10.21883/OS.2020.10.50019.161-20>
30. Гаврилова Н.Д., Мальшикина И.А. Влияние изменений в структуре сетки водородных связей воды на электрофизические свойства систем «матрица-вода» при ступенчатом нагреве. *Вестник Московского университета. Серия 3. Физика. Астрономия.* 2018;(6):74–80. URL: <http://vmu.phys.msu.ru/file/2018/6/18-6-074.pdf>

29. Krauklis I.V., Tulub A.V., Golovin A.V., *et al.* Raman spectra of glycine and their modeling in terms of the discrete–continuum model of their water solvation shell. *Opt. Spectrosc.* 2020;128(10):1598–1601. <https://doi.org/10.1134/S0030400X20100161>

[Original Russian Text: Krauklis I.V., Tulub A.V., Golovin A.V., Chelibanov V.P. Raman spectra of glycine and their modeling in terms of the discrete–continuum model of their water solvation shell. *Optika i Spektroskopiya.* 2020;128(10):1488–1491 (in Russ.). <https://doi.org/10.21883/OS.2020.10.50019.161-20>]

30. Gavrilova N.D., Malyshkina I. A. The influence of changes in the structure of hydrogen bonds of water on the electrophysical properties of matrix-water systems in stepwise heating. *Moscow Univ. Phys.* 2018;73(6):651–658. <https://doi.org/10.3103/S0027134918060127>

[Original Russian Text: Gavrilova N.D., Malyshkina I. A. The influence of changes in the structure of hydrogen bonds of water on the electrophysical properties of matrix-water systems in stepwise heating. *Vestnik Moskovskogo Universiteta. Seriya 3. Fizika. Astronomiya.* 2018;(6):74–80 (in Russ.). URL: <http://vmu.phys.msu.ru/file/2018/6/18-6-074.pdf>]

About the authors:

German O. Stepanov, Cand. Sci. (Biol.), Senior Research, Materia Medica Holding, (47-1, Trifonovskaya ul., Moscow, 129272, Russia). E-mail: stepanovgo@materiamedica.ru. Scopus Author ID 15046034100, <https://orcid.org/0000-0002-8576-9745>

Natalia N. Rodionova, Cand. Sci. (Biol.), Head of Physicochemical Research, Materia Medica Holding, (47-1, Trifonovskaya ul., Moscow, 129272, Russia). E-mail: rodionovann@materiamedica.ru. <https://orcid.org/0009-0001-7138-9063>

Roman R. Konstantinov, Researcher, Materia Medica Holding, (47-1, Trifonovskaya ul., Moscow, 129272, Russia). E-mail: konstantinovrr@materiamedica.ru. <https://orcid.org/0009-0000-6692-2583>

Kirill A. Subbotin, Cand. Sci. (Eng.), Head of the Department of Laser Crystals and Solid-State Lasers, Prokhorov General Physics Institute, Russian Academy of Sciences (38, Vavilova ul., Moscow, 119991, Russia); Associate Professor, Department of Chemistry and Technology of Crystals, Mendeleev University of Chemical Technology of Russia (9, Miusskaya pl., Moscow, 125047, Russia). E-mail: soubbot1970@gmail.com. Scopus Author ID 6701562918, RSCI SPIN-code 7976-1488, <https://orcid.org/0000-0001-9590-7403>

Об авторах:

Степанов Герман Олегович, к.б.н., ведущий научный сотрудник, ООО «НПФ «Материя Медика Холдинг» (129272, Россия, Москва, ул. Трифоновская, д. 47, стр. 1). E-mail: stepanovgo@materiamedica.ru. Scopus Author ID 15046034100, <https://orcid.org/0000-0002-8576-9745>

Родионова Наталья Николаевна, к.б.н., руководитель физико-химических исследований, ООО «НПФ «Материя Медика Холдинг» (129272, Россия, Москва, ул. Трифоновская, д. 47, стр. 1). E-mail: rodionovann@materiamedica.ru. <https://orcid.org/0009-0001-7138-9063>

Константинов Роман Романович, научный сотрудник, ООО «НПФ «Материя Медика Холдинг» (129272, Россия, Москва, ул. Трифоновская, д. 47, стр. 1). E-mail: konstantinovrr@materiamedica.ru. <https://orcid.org/0009-0000-6692-2583>

Субботин Кирилл Анатольевич, к.т.н., заведующий отделом лазерных кристаллов и твердотельных лазеров, ФГБУН ФИЦ «Институт общей физики им. А.М. Прохорова Российской академии наук» (119991, Россия, Москва, ул. Вавилова, д. 38); доцент кафедры химии и технологии кристаллов, ФГБОУ ВО «Российский химико-технологический университет им. Д.И. Менделеева» (125047, Россия, Москва, Миусская пл. д. 9). E-mail: soubbot1970@gmail.com. Scopus Author ID 6701562918, SPIN-код РИНЦ 7976-1488, <https://orcid.org/0000-0001-9590-7403>

The article was submitted: October 06, 2023; approved after reviewing: November 03, 2023; accepted for publication: November 24, 2023.

*Translated from Russian into English by H. Moshkov
Edited for English language and spelling by Dr. David Mossop*